The 11th Canadian Conference on Earthquake Engineering
Canadian Association for Earthquake Engineering
11CCEE

SEISMIC EVALUATION AND RETROFIT OF MASONRY BUILDINGS

Murat SAATCIOGLU
Professor and University Research Chair in Earthquake Engineering, University of Ottawa, Ottawa, Canada
Murat.Saatcioglu@uOttawa.ca

Ken ELWOOD
Professor and MBIE Chair in Earthquake Engineering, University of Auckland, New Zealand
k.elwood@auckland.ac.nz

ABSTRACT: A review of seismic evaluation procedure outlined in ASCE41-13 is presented with emphasis on masonry buildings. Research projects conducted on seismic performance and retrofit of masonry walls are summarized. Retrofit techniques developed for masonry load bearing walls, consisting on surface-mounted carbon fibre reinforced polymer (CFRP) sheets, with CFRP anchors, as well as with stainless steel sheet anchors are presented. It is illustrated that the use of CFRP sheets is an effective retrofit technique to suppress shear distress in masonry walls. The use of appropriate anchors, providing tension ties to adjoining members can improve flexural wall resistance significantly. These techniques are able to improve both strength and deformation capacities to levels that can meet the required performance objectives outlined in ASCE41-13. The retrofit of unreinforced masonry (URM) infill panels with CFRP diagonal elements, properly anchored to the enclosing frame members can result in strength and stiffness enhancements in seismically deficient non-ductile reinforced concrete frames. The out-of-plane performance of URM walls are affected with the flexibility of top and bottom diaphragms and should be considered in retrofit design.

1. Introduction

This paper presents an overview of seismic evaluation procedures for masonry buildings outlined in ASCE41-13 (ASCE, 2013), followed by a summary of research conducted on seismic performance and retrofit of masonry buildings within the scope of the Canadian Seismic Research Network. The emphasis is placed on performance, evaluation and retrofit of load bearing unreinforced and partially reinforced masonry walls, as well as unreinforced masonry (URM) infill walls in reinforced concrete frames. Both in-plane and out-of-plane behaviour of masonry walls are addressed.

2. Overview of ASCE41-13 Requirements for Seismic Evaluation of Masonry Buildings

2.1. Performance Objectives and Seismic Hazards

ASCE Standard on Seismic Evaluation and Retrofit of Existing Building (ASCE41, 2013) provides a three-tier approach for seismic evaluation of buildings located in regions of different seismicity. The evaluation of buildings is done for a selected Performance Objective, which consists of a selected Hazard Level and Target Structural and Non-structural Performance Levels. Different combinations of hazards and performance levels result in different Building Performance Objectives.

***Seismic Hazard Levels*:** Seismic hazard is defined as acceleration response spectra or acceleration ground motion records for the location under consideration. The ASCE41-13 specifies four basic hazard levels as “Basic Safety Earthquakes (BSE).” Two are intended for new buildings (BSE-1N and BSE-2N)

and the other two are for existing buildings (BSE-1E and BSE-2). Seismic Hazard Level BSE-2N is intended to match the design ground motions specified in ASCE-7 for the design of new buildings. The design of new buildings in Canada conforms to the National Building Code of Canada (NRC, 2010) with an earthquake hazard level equal to 2% of probability of exceedance in 50 years. This hazard level can be adopted for BSE-2N. The Hazard Level BSE-1N is equal to 2/3rd of BSE-2N and can be viewed as being equivalent to 10% probability of exceedance in 50 years. Basic Safety Earthquakes for use with Basic Performance Objectives for Existing Buildings are defined as BSE-2 with 5% probability of exceedance in 50 years and BSE-1 with 20% probability of exceedance in 50 years.

Target Building Performance Levels: Target Building Performance Levels consist of a combination of Target Structural and Non-Structural Performance Levels. The Structural Performance Levels consist of 6 discrete levels and two intermediate ranges. The discrete levels are; i) Immediate Occupancy (S-1), ii) Damage Control (S-2), iii) Life Safety (S-3), iv) Limited Safety (S-4), v) Collapse Prevention (S-5) and vi) Not Considered (S-6). Immediate Occupancy indicates a post-earthquake damage state in which the building remains safe to be re-occupied with essentially the same strength and stiffness as those prior to the earthquake. Life Safety is defined as the post-earthquake damage state where damage to some structural components are inflicted, but the structure retains a margin of safety against partial or total collapse. Damage control state is taken as the mid-point of the range between immediate occupancy and life safety sates of damage. Collapse Prevention is defined as a damage state in which a structure has damaged elements but maintain its gravity load carrying capacity without any margin of safety against collapse. The Limited Safety Performance Level corresponds to a damage state half way between Life Safety and Collapse Prevention. If the assessment of a building does not involve any structural component, as in the case of seismic retrofit of non-structural components, then the Structural Performance Level is specified as “Not Considered.”

The intermediate Structural Performance Ranges are Enhanced Safety Structural Performance Range, which is taken as the range between the Immediate Occupancy and Life Safety Performance Levels; and the Reduced Safety Structural Performance Range, which is between the Life Safety and Collapse Prevention Levels.

Target Non-structural Performance Levels are selected from four discrete levels, consisting of; i) Operational (N-A), ii) Position Retention (N-B), iii) Life Safety (N-C) and iv) Not Considered (N-D). Operational Non-structural Performance Level implies that the non-structural members continue functioning after the earthquake to fulfill their intended functions before the earthquake. Position Retention Non-structural Performance Level indicates damage to non-structural components to a point where they are no longer functional, but they are sufficiently secured to prevent further damage that may be caused by falling, toppling and breakage of utility connections. However, access to the building (doors and windows), stairways and elevators remain functional. Life Safety non-structural Performance Level is the damage state in which non-structural components may be significantly damaged, but they do not threaten life safety. When the evaluation and retrofit of a building does not address non-structural components, then the Non-structural Performance Level Not Considered applies.

Performance Objectives: Performance objectives consist of a combination of Target Building Performance Levels and Hazard Levels. Four Performance Objectives are defined in ASCE41-13; i) Basic Performance Objective for Existing Buildings (BPOE), ii) Enhanced Objectives, iii) Limited Objectives, and iv) Basic Performance Objective Equivalent to New Building Standard (BPON). They vary with Risk Categories. Though ASCE41-13 does not assign Risk Categories to buildings, it identifies the components of Performance Objectives necessary to conduct building evaluation for a specified level of risk. Risk is left to the building owner together with seismic assessment professionals and regulatory authorities to define, while the ASCE41-13 procedure identifies what level of assessment is needed to fulfill a specific Performance Objective for a pre-determined Risk Level. A three-tier assessment procedure is specified, each covering a different level of sophistication in terms of computational and analytical efforts; as i) Tier 1, ii) Tier 2 and iii) Tier 3. Tier 1 involves seismic screening, and helps identify buildings that comply with a specific Performance Objective. It can be implemented with relatively small effort. It utilizes various checklists without much computational effort. This process identifies deficiencies in buildings, if any. The deficiencies identified as “Noncompliant,” or buildings components that do not respond to Tier 1 checklists (hence deemed to be “Unknown”) require further evaluation. This is done through Tier 2 deficiency-based evaluation. This level of assessment need not expand beyond those

elements that have been identified as non-compliant by the Tier 1 assessment. Tier 2 involves a more detailed evaluation of the specific components that was found to be deficient or a component for which sufficient information could not be gathered in Tier 1 checklists. An assessment of the entire building may be needed for some buildings. In this case Tier 3 assessment process is employed. Tier 3 involves an analysis of the entire building, either in its existing condition or after the retrofit measures have been implemented. It brings in all the sophistications of detailed analysis, and hence requires judgement before its need can be justified. This decision should be based on whether Tier 1 and Tier 2 evaluations have resulted in too conservative outcomes or whether there would be significant economic of performance advantages for more detailed and sophisticated evaluation. ASCE41-13 clearly identifies the analysis procedures and the assessment methodologies suitable for each tier of evaluation. Table 1 summarizes target performance levels to be checked under specific hazard levels to fulfill the requirements of Basic Performance Objectives for Existing Buildings (BPOE) for different pre-determined Risk Levels and different levels of sophistication in the assessment procedure (as Tier 1, Tier 2 and Tier 3).

Table 1 – Basic Performance Objective for Existing Buildings (BPOE)(ASCE41, 2013)

	Tier 1[a]	Tier 2[a]	Tier 3	
Risk Category	BSE-1E	BSE-1E	BSE-1E	BSE-2E
I & II	Life Safety Structural Performance Life Safety Nonstructural Performance (3-C)	Life Safety Structural Performance Life Safety Nonstructural Performance (3-C)	Life Safety Structural Performance Life Safety Nonstructural Performance (3-C)	Collapse Prevention Structural Performance Nonstructural Performance Not Considered (5-D)
III	See footnote *b* for Structural Performance Position Retention Nonstructural Performance (2-B)	Damage Control Structural Performance Position Retention Nonstructural Performance (2-B)	Damage Control Structural Performance Position Retention Nonstructural Performance (2-B)	Limited Safety Structural Performance Nonstructural Performance Not Considered (4-D)
IV	Immediate Occupancy Structural Performance Position Retention Nonstructural Performance (1-B)	Immediate Occupancy Structural Performance Position Retention Nonstructural Performance (1-B)	Immediate Occupancy Structural Performance Position Retention Nonstructural Performance (1-B)	Life Safety Structural Performance Nonstructural Performance Not Considered (3-D)

[a]For Tier 1 and 2 assessments, seismic performance for the BSE-2E is not explicitly evaluated.
[b]For Risk Category III, the Tier 1 screening checklists shall be based on the Life Safety Performance Level (S-3), except that checklist statements using the Quick Check procedures of Section 4.5.3 shall be based on MS-factors and other limits that are an average of the values for Life Safety and Immediate Occupancy.

Buildings retrofitted to meet the requirements of BPOE have a lower level of safety and higher risk of damage and collapse potential than the new buildings designed to current codes of practice. However, there are reasons for accepting a somewhat greater risk in existing buildings. It is generally accepted that the cost of achieving higher safety through more rigorous retrofitting is often disproportionate to the incremental benefits achieved. Existing building often have less number of years left in their economic life, as compared to new buildings, which are designed based on a 50-year economic life, with earthquake probabilities of occurrences defined for this period, implying that the chances of older buildings seeing a code design level earthquake would be lower. Furthermore, meeting the new code requirements may render the building unsafe shortly after it is built if the code requirements were to change. Sometimes a reduced safety level than that is inferred by BPOE may be deemed sufficient for the Risk Category considered. In this case building assessment is conducted to meet the Reduced Performance Objective. In this case seismic evaluation is conducted either under lower hazard levels than BSE-1E and BSE-2E, or Target Structural and Non-structural Performance Levels are taken to be less than those for the BPOE. Alternatively, the BPOE can be used with a lower Risk Category. Conversely, sometimes a seismic evaluation before or after retrofit demonstrates higher performance than that outlined for the BPOE. This happens when the assessment is done either under higher Hazard Levels than BSE-1E and BSE-2E or the Structural and Non-structural Performance Levels attained exceed those expected for the BPOE. Alternatively, the latter may exceed the performance requirements associated with the selected Risk Level. In such cases the building is deemed to meet Enhanced Performance Objectives.

Sometimes it may be required to upgrade a building to the current design code levels intended for new buildings. In such cases, the evaluation and retrofit objectives should meet Basic Performance Objective Equivalent to New Building Standards (BPON). The BPON is intended specifically for Tier 3 systematic evaluation or retrofit. Table 2 summarizes the BPON, which includes an assessment at the code hazard level. In Canada this hazard level corresponds to design earthquakes with 2% probability of exceedance as outlined in the National Building Code of Canada (NRC, 2010).

Table 2 – Basic Performance Objective Equivalent to New Building Standards (BPON) (ASCE41, 2013)

Risk Category	Seismic Hazard Level	
	BSE-1N	BSE-2N
I & II	Life Safety Structural Performance Position Retention Nonstructural Performance (3-B)	Collapse Prevention Structural Performance Nonstructural Performance Not Considered (5-D)
III	Damage Control Structural Performance Position Retention Nonstructural Performance (2-B)	Limited Safety Structural Performance Nonstructural Performance Not Considered (4-D)
IV	Immediate Occupancy Structural Performance Operational Nonstructural Performance (1-A)	Life Safety Structural Performance Nonstructural Performance Not Considered (3-D)

2.2. Evaluation and Retrofit of Masonry Components

Once performance objectives are defined for the building at hand, seismic evaluation is conducted to identify any potential deficiency for possible retrofitting. The first step in the evaluation involves condition assessment and data collection to establish material properties in the existing building. The structural components in buildings are classified as “Primary” and “Secondary Components. Those that are required to resist seismic forces while accommodating deformations to achieve selected performance Levels are classified as “Primary Components,” whereas those accommodate the same deformations without having the requirement to resist seismic forces are classifies as “Secondary Components.” The condition assessment is first conducted for both primary and secondary components and their condition is classified as Good, Fair or Poor. This can be done ether by visual inspection or through a comprehensive condition assessment which may involve non-destructive tests. The details of condition assessment and data collection for material properties are outlined in ASCE41-13.

Analysis of masonry buildings is performed by using one of the four methods specified; i) linear static procedure (LSP), ii) linear dynamic procedure (LDP), iii) nonlinear static procedure (NSP), and iv) nonlinear dynamic procedure (NDP). The strength is established by assuming either force-controlled or deformation controlled actions. Strengths used in design for force-controlled actions (Q_{CL}) are computed as lower bound strength values, corresponding to mean minus one standard deviation. Strengths used for deformation-controlled actions (Q_{CE}) are taken as the mean maximum resistance expected over the entire range of deformations the member is expected to experience. The strength values can be established either by following the principles of mechanics, or experimentally. The strength design procedure may be used with a capacity reduction (or material resistance) factor ϕ = 1.0. When a nonlinear procedure is employed to compute strength values, component force-deformation relationships, obtained either experimentally or the generalized force-deformation relationship shown in Fig. 1 can be used, with parameters c, d, e, and f as defined in ASCE41-13. The force-deformation relationship shown in Fig 1(b)

should be used for elements that show brittle characteristics. The lateral drift and wall height considered in Fig. 1 are explained in Fig. 2 graphically. The stiffness of masonry walls should include the effects of flexure, shear and axial deformations.

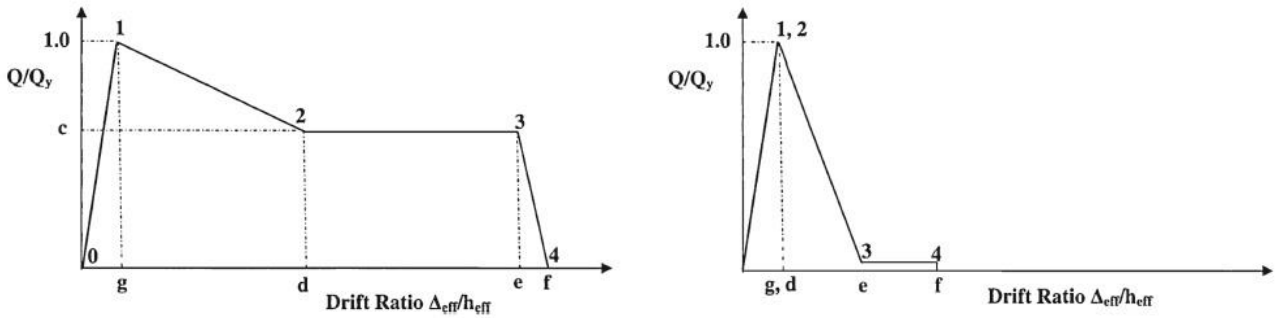

a) Deformation-Controlled Actions **b) Force-Controlled Actions**

Fig. 1 – Typical Generalized Force-Deformation Relationships for Reinforced and Unreinforced Masonry (ASCE41, 2013)

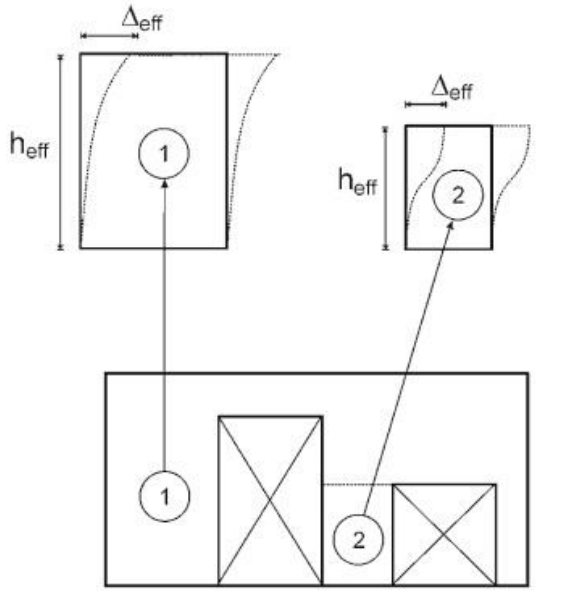

Fig.2 – Effective Height and Differential Displacement of Wall Components (ASCE41, 2013)

URM load bearing walls and wall piers subjected to in-plane actions develop five primary actions. Forced-controlled in-plane actions include; i) toe crushing, ii) diagonal tension that generates diagonal cracks through masonry units, and iii) vertical compression. Deformation controlled in-plane actions include; i) rocking and ii) bed-joint sliding, including stair-step cracking through head and bed joints. ASCE41-13 provides expressions for the evaluation of strength governed by each of these actions. In-plane shear

action in URM walls is considered to be a deformation-controlled action if shear resistance to rocking and bed-joint sliding is lower than the lateral strength of the wall or the wall pier in toe crushing, diagonal tension and vertical crushing. Acceptance criteria for rocking and sliding are specified in ASCE41-13. For URM walls with rocking and sliding governing modes, values for expected ductility and drift ratios associated with each performance level are specified. Reinforced Masonry (RM) walls are evaluated in much the same manner as URM walls, except for the consideration of inherent flexural ductility. Both linear and non-linear methods of analyses can be employed with appropriate modelling of force-deformation relationships for ductile and brittle elements as illustrated in Fig. 1. ASCE41-13 provides acceptance criteria for linear and non-linear procedures based on expected ductility factors (m-factors) and acceptable drift limits for all performance levels.

The out-of-plane URM and RM walls are also required to be assessed against out-of-plane actions. Such assessment cannot be conducted under static loads, whether linear or non-linear. Dynamic analysis is required for proper considerations of inertia effects. ASCE 41-13 provides Structural Performance Limits for walls subjected to out-of-plane actions, with permissible height to thickness ratios to control stability failures.

3. Research on Performance and Retrofit of Masonry Walls

A number of research projects were conducted within the scope of the Canadian Seismic Research Network on seismic performance and retrofit of masonry walls. Highlights of some of these research projects are presented in the following sections. More specifically, strength and ductility improvements obtained in load bearing URM and Partially Reinforced Masonry (PRM) walls, as well as in-plane strengthening of URM infill panels are presented. In addition, a comprehensive research project conducted on out-of-plane behaviour of masonry walls is summarized.

3.1. Retrofit of Masonry Load Bearing Walls

Experimental research was conducted at the Structures Laboratory of the University of Ottawa to improve strength and deformability of masonry load bearing walls. These walls, especially in existing older construction, lack sufficient strength and deformability to meet the Basic Performance Objectives for Existing Buildings (BPOE) discussed in Sec. 2.1. Two pairs of walls were designed and tested under incrementally increasing lateral deformation reversals (Taghdi et al., 2000). The first pair consisted of unretrfoitted URM and PRM walls, built using 200 mm concrete blocks, having 2.0 m height and 2.0 m length. Figure 3 illustrates the walls during construction. They were built on a heavily reinforced concrete footing, which was fixed to the laboratory strong floor. A loading beam was placed on the wall for the application of lateral deformation reversals by means of a 1000 kN capacity MTS Actuator. The geometry of the unretrfoitted walls is shown in Fig. 4(a). The walls were tested under a constant axial load of 100 kN, which was applied by two vertically positioned MTS actuators. The test setup is illustrated in Fig. 4(b).

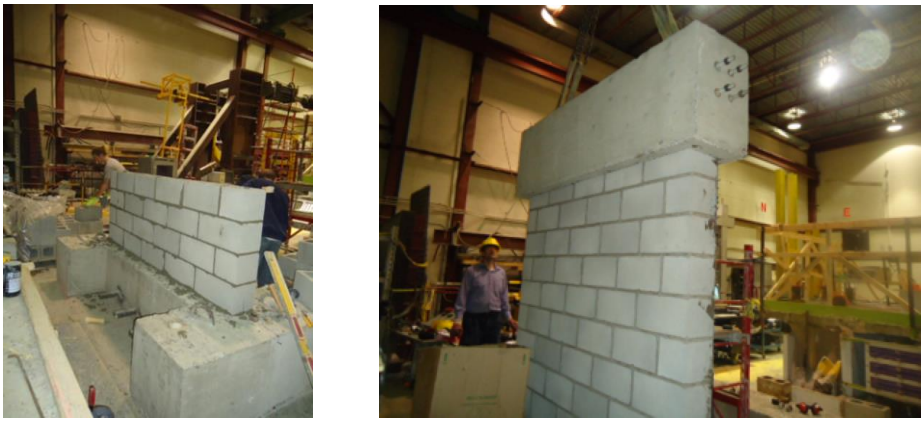

Fig. 3 – Masonry walls during construction

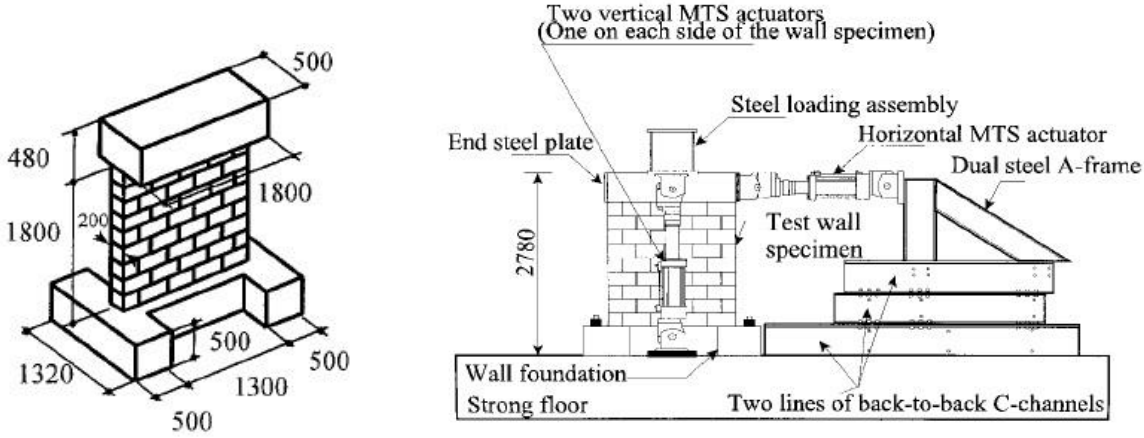

a) Wall Geometry b) Test set-up

Fig. 4 – Geometry and test setup used for unretrofitted wall tests

The URM wall behaved in a combination of rocking and sliding mode. The sliding developed in one direction during the push cycles at an ultimate force of 65 kN. Rigid body rocking was observed with slight sliding when the wall was subjected to pull cycles at an ultimate force of -59 kN. The wall exhibited relatively large deformations with minor strength decay before failure. Rocking and sliding was observed to occur along the bed joint above the second course of blocks. Figure 5 illustrates the observed rocking and sliding behaviour schematically. Rocking started at about 0.8% lateral drift cycles. The hystertic behaviour is shown in Fig 6, indicating limited strength and deformability.

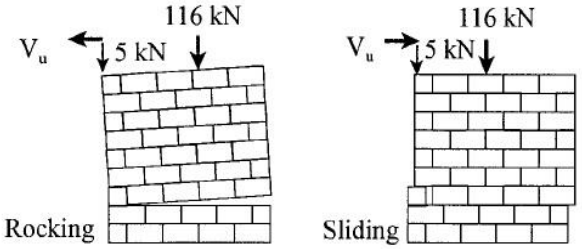

Fig. 5 – Rocking and Sliding in URM wall

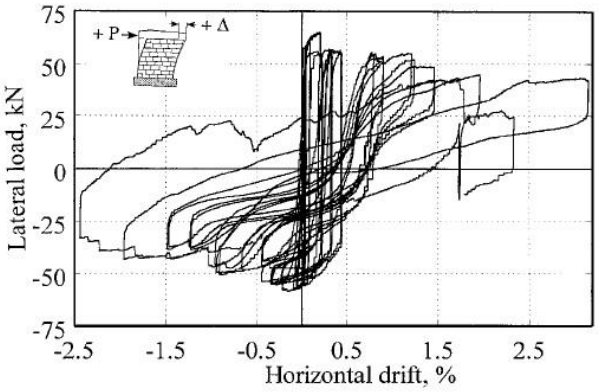

Fig. 6 – Hysteretic relationship of URM Wall

The second wall in the pair was unretrfoitted partially reinforced masonry (PRM) wall. It had the same geometry as the URM wall, details of which are shown in Fig. 4(a). The reinforcement details of the wall are given in Fig. 7. The PRM wall was tested by following the same loading protocol under incrementally increasing lateral deformations under a constant axial compression of 100 kN. The hysteretic relationship shown in Fig. 8 indicates symmetric and relatively fat hysteresis loops. The wall developed higher strength than the companion URM wall, but suffered from shear failure. Diagonal compression struts resulted in progressive crushing of masonry units, leading to early strength decay. The deformation capacity, prior to developing significant strength decay was approximately 0.4%. During testing, cracks appeared along vertical and horizontal mortar joints, between the diagonal corners, forming a stair-step pattern at about 50% of the wall capacity. The vertical reinforcement did not yield and the wall could not develop its flexural capacity due to the crushing of diagonal compression struts. The wall in-plane capacity was limited to approximately 120 kN, after which gradual crushing of the masonry was observed.

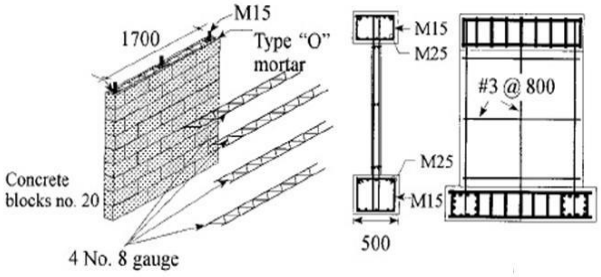

Fig. 7 – Reinforcement details of PRM Wall

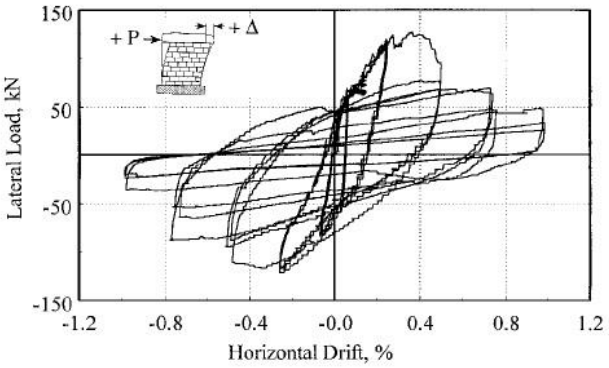

Fig. 8 – Hysteretic Relationship for PRM Wall

The second pair of walls was companion to the URM and PRM walls described above with seismic retrofitting (Arifuzzaman, 2013). The retrofit strategy adopted was to increase shear capacity by applying surface-bonded carbon fibre reinforced polymer (CFRP) sheets, while also increasing the flexural capacity by providing continuity between vertically aligned carbon fibres and the foundation. The walls were externally reinforced by means of two CFRP sheets applied on one side, to simulate practical scenarios in which the wall may not be accessible from both sides. One ply of CFRP sheet was applied vertically and another ply was applied horizontally. Each ply formed 1.0 mm thick laminate, having a tensile strength of 780 MPa for the composite material (fibres plus epoxy), with a rupturing strain of 1.2%. The retrofitted walls were tested in the same manner as the previous two unretrofitted companion walls. This time however, the axial load of 100 kN was applied by means of prestressing strands.

The flexural strength of the retrofitted URM wall was ensured by means of using ductile steel sheet anchors, provided near wall ends, on one side of the wall. The steel anchors were manufactured from stainless steel sheets of 1.2 mm thickness. The steel had 300 MPa yield capacity, exhibiting well-rounded post yield characteristics, with 620 MPa tensile rupturing capacity. An important aspect of the stainless steel was its extremely high elongation characteristics. The steel sheet showed 60% elongation before it ruptured in tension. The plates were cut to have a 400 mm width on the wall side, and a reduced width of 300 mm in the foundation, below the wall panel, to promote yielding at the wall-foundation interface. They were bonded on masonry and concrete through the application of epoxy. The larger surface area on the wall, improved bond between the steel plate and the wall panel. Figures 9 and 10 Illustrate a typical stainless steel sheet anchor and the retrofitted URM wall specimen. Figure 11 shows the implementation of the retrofit scheme.

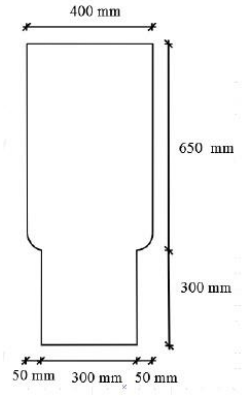

Fig. 9 – Steel Sheet Anchor

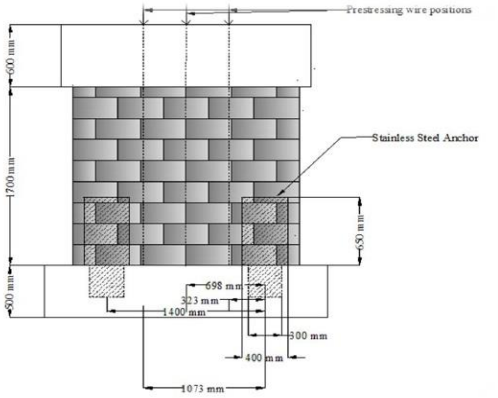

Fig. 10 – URM Wall Retrofitted with Steel Sheet Anchors

a) Cutting of the foundation concrete

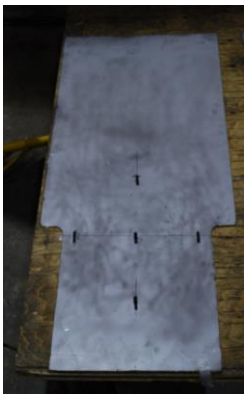

b) Steel Sheet Anchor

c) Anchor Placement

d) Anchors on the Wall Surface

e) Anchors covered by a Layer of CFRP

Fig. 11 Implementation of Ductile Stainless Steel Sheet Anchors

The application of CFRP sheets completely eliminated diagonal tension cracks and prevented shear failure. The application of the steel sheet anchors provided the required tension reinforcement between the foundation and the wall panel, and transferred tensile forces from the foundation to the vertical carbon fibres in CFRP. This resulted in substantial flexural capacity. The wall behaved in a ductile flexural mode. The steel sheet anchored yielded and developed very high elongations without experiencing tension rupturing. However, load reversals caused local buckling of the anchor sheets in compression. This resulted in pinching of hysteresis loops. The hysteretic relationship recorded during the test is shown in Fig. 12(a). As can be seen, relative to the unretrofitted URM wall, there was a four-fold increase in lateral load capacity, with increased ductility. The test was stopped because the actuator stroke capacity was exceeded in the push side. It was then decided to continue the test with the application of pull cycles only up to 4.2% lateral drift ratio, as shown in Fig. 12(b), at which level the stroke capacity of the actuator was exceeded in the pull direction as well. There was no strength degradation observed during the test.

The companion PRM wall was retrofitted with CFRP sheets and CFRP anchors for both shear and flexure enhancement. The surface bonded CFRP was applied in much the same manner as before, in two plies, one in each direction; but this time the ply with vertical fibres extended towards the foundation, folded over the foundation concrete and anchored by means of CFRP anchors that were developed earlier (Ozbakkaloglu and Saatcioglu 2009). These anchors were used to provide additional anchorage of the FRP to the foundation concrete. The same anchors were also used on wall surface along the wall diagonals to improve bond between FRP and masonry surface, to help resist diagonal tension. The anchor details are shown in Fig. 13.

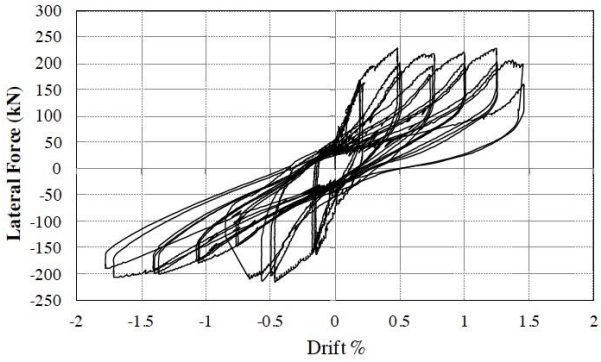

a) Hysteretic Force-Deformation Relationship

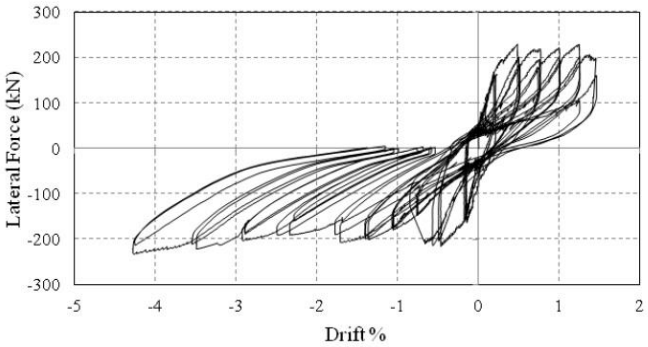

b) Hystertic Relationship with Continued Pull Cycles

Fig. 12. – Recorded Hysteretic relationships for Retrofitted URM Wall

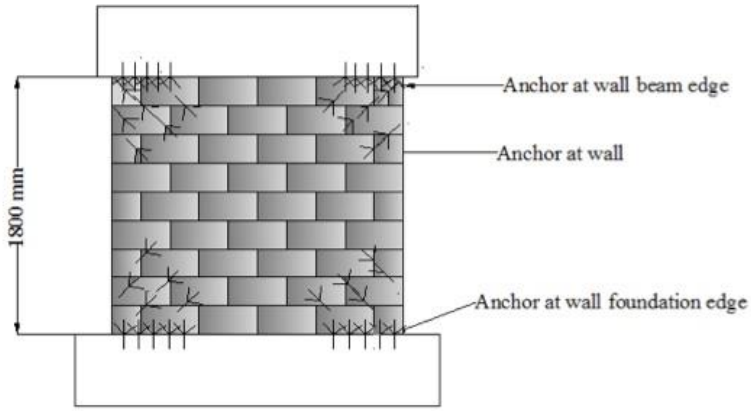

a) FRP Anchor Details

b) CFRP Vertical Ply Folded over Foundation for Continuity

c) CFRP Anchor

d) Close up View of Installed CFRP Anchors

e) Retrofitted PRM Wall during Testing

Fig. 13 – The CFRP Anchor Details used for Retrofitting PRM Wall

The wall reached its maximum lateral load resistance of 165 kN and 174 kN in push and pull during 0.5% drift cycles. At this stage of loading the internal steel reinforcement yielded. The lateral load capacity was limited by debonding of the FRP from the foundation, followed by the pull-out of the extreme tension

anchors from the foundation. Pull-out of the remaining CFRP anchors was observed during the subsequent 0.75% drift cycles in the push direction. This resulted in a drop of lateral load resistance to 138 kN. The wall continued resisting increased force resistance during the pull cycles, reaching 182 kN at 0.75%. However, the CFRP anchors on the tension side started pulling out at about 1% pull cycles and the load dropped to 120 kN. The deformation cycles at 2.5% drift resulted in masonry toe crushing near the east end when the load was in the push direction. The internal #15M bars and the compression resistance of masonry resulted in reduced wall capacity until after 4% lateral drift. The hystertic relation recorded during the test is shown in Fig. 14. It was observed after the test that some of the CFRP anchors had not been fully inserted to have the full required 100 mm of embedment depth, hence did not develop their full capacities.

The tests indicated that the two retrofit techniques employed for URM and PRM walls were able to improve strength and deformability of masonry walls, and can be used to meet retrofit performance objectives of otherwise deficient bearing walls.

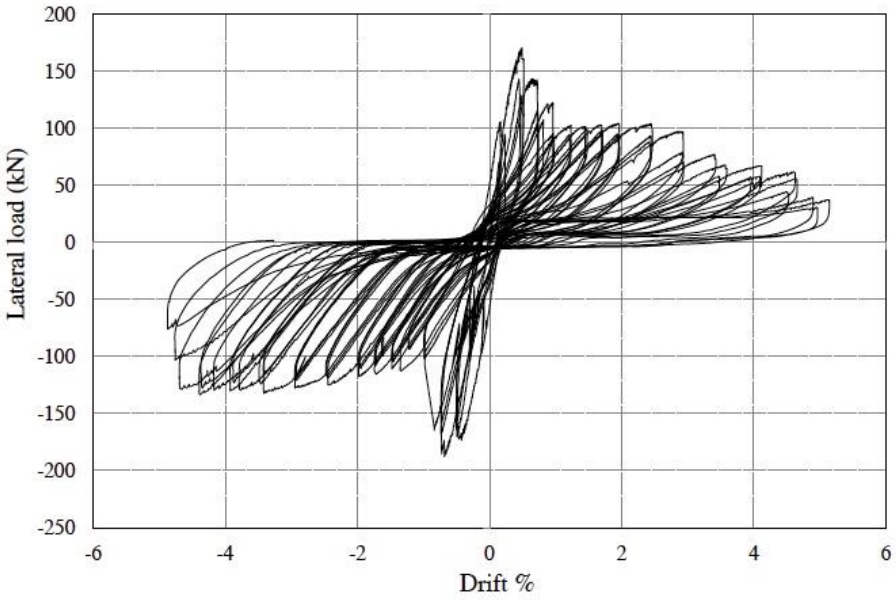

Fig. 14 – Hysteretic Relationship of Retrfoitted PRM Wall

3.2. Retrofit of Masonry Infill Walls in Reinforced Concrete Frames

Another experimental research project was conducted at the Structures Laboratory of the University of Ottawa to improve the performance of non-ductile reinforced concrete frames with concrete block masonry infill panels (Saatcioglu et al., 2005). Three half-scale reinforced concrete frames were designed on the basis of the ACI 318 (1963) Building Code to simulate older existing building frames. The frames were constructed and the masonry walls were built to be tested under uniformly distributed gravity loads and incrementally applied lateral deformation reversals. The first specimen (BL-1) was built to reflect the majority of existing buildings constructed prior to the 1970's, with a gravity-load designed frame. Figure 15 illustrates the details of the specimen. A professional contractor was hired to build the masonry infills to implement the actual practice in industry. Two additional companion specimens were built for retrofitting with CFRP sheets. Two aspects of the retrofit strategy were of concern; i) the amount and arrangement of CFRP sheets and ii) the possibility of debonding of sheets and measures against them. It was decided to retrofit one of the walls (BL-2) with two layers of CFRP sheets per face, covering the entire wall surface, where each layer was oriented such that the fibers were parallel to one of the diagonal as shown in Figure 16(a), and the other layer was oriented to have the fibers parallel to the opposite diagonal. This resulted in four layers of sheets, two per wall face. The diagonal orientation of fibers was selected to increase their efficiency since their primary function was to resist diagonal tension. The other specimen was retrofitted with diagonal strips of CFRP sheets, creating an X pattern, as illustrated in Figure 16(b). Two sheets of CFRP were used on each side, one sheet along each diagonal, and the other

along the opposite diagonal. Two additional strips were used on the other side of the wall, creating symmetric retrofitting, resulting in a total of four strips, two in each direction. The strip width was equal to 625 mm.

Specially designed CFRP anchors were developed and used to minimize/eliminate the delamination of CFRP sheets from the surface of the wall (Ozbakkaloglu and Saatcioglu 2009). This was done by drilling holes in frame members adjacent to the wall with approximately 45-degree inclination towards the centre of the frame elements, and inserting the anchors to be epoxy glued into the concrete. The anchors were produced in the Laboratory by twisting strips of CFRP sheets and folding into two, as illustrated in Fig. 17 (a). A hammer drill was used to make approximately 50 mm deep, 12 mm diameter holes in columns and beams for the FRP anchors, as shown in Figure 17(b). Wooden pieces were inserted into the anchor holes during the placement of CFRP sheets, as guides, and also to avoid filling of the holes with epoxy. This is illustrated in Fig. 17(c). The anchors were placed and epoxy glued after the application of surface bonded CFRP sheets, as depicted in Figure 17(d).

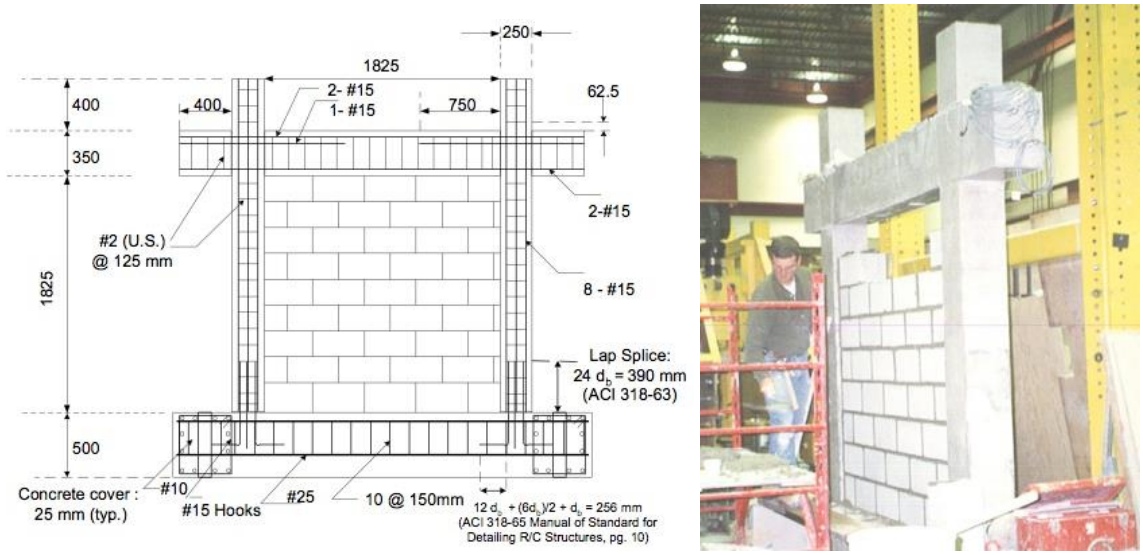

(a) (b)

Fig. 15 – Infilled Frame (BL-1), (a) Geometric Details, (b) Wall under Construction

(a) (b)

Fig. 16 – FRP Retrofitted Walls, (a) Specimen BL-2, (b) Specimen BL-3

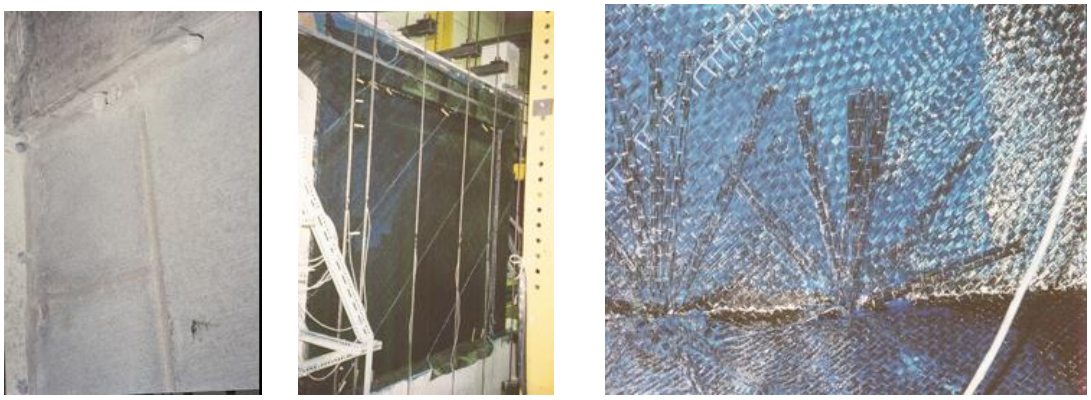

(a) (b) (c)

Fig. 17 – Installation of CFRP anchors, (a) Pre-drilled holes, (b) Wooden guides, (c) Anchors in place

The specimens showed a significant participation of the walls in the frame response. The walls were able to stiffen the frames during the initial stages of loading. Specimen BL-1, without the retrofit, experienced gradual stiffness degradation under reversed cyclic loading. Progressive cracking of masonry units and mortar joints led to the dissipation of energy, without affecting the strength of the frame. The lateral drift was controlled by the stiffening effect of the wall. Of particular interest was the simultaneous degradation of strength and stiffness of the wall and the frame, contrary to the belief that the masonry walls would disintegrate early in seismic response, leaving the frames as the only structural system to resist earthquakes. This may be the characteristic of the wall system tested, as the wall was constructed to be in full contact with the frame. However, it does indicate that the two materials, i.e., reinforced concrete and infill masonry are compatible in resisting lateral forces unless the infill panles experience out-of-plane failures. The initial resistance was provided mostly by the wall. The load resistance was gradually transferred to the frame through progressive cracking and softening of the wall. The eventual failure of the unretrofitted specimen was caused by the hinging of columns within the reinforcement splice regions near the ends, while a significant portion of the cracked infill wall remained intact. Figure 18 shows the hysteretic force-lateral drift relationship of the unretrofitted frame-wall assembly. The relationship indicates that the peak load of 273 kN was attained in the direction of first load excursion at approximately 0.25% lateral drift ratio and remained constant up to about 1% drift, though there was substantial stiffness degradation during each cycle of loading. Gradual strength decay was observed after 1% drift, and the assembly failed due to the failure of concrete columns in their reinforcement splice regions at about 2% lateral drift ratio.

The retrofitted specimens showed a substantial increase in the elastic rigidity and strength. The initial slope of the force-deformation relationship was high, corresponding to that of uncracked wall stiffness and remained at the uncracked stiffness level until the specimens approached their peak resistances. This was especially true for specimen BL-2 where the entire wall surface was covered with FRP sheets. It was clear that the FRP control of cracking helped improve the wall rigidity. Speciemn BL-2 resisted a peak load of 784 kN in the direction of first load excursion, indicating an improvement of approximately a factor of 3. The peak load was attained at approximately 0.3% lateral drift ratio. The FRP sheets maintained their integrity until after the peak resistance was reached. There was no debonding observed throughout the test. However, the FRP sheets started rupturing gradually near the opposite corners in diagonal tension. This resulted in strength decay. By about 0.5% lateral drift, approximately 25% of the peak load resistance was lost. The load resistance continued to drop during subsequent deformation reversals and the resistance dropped to the level experienced by the unretrofitted specimen at approximately 1% drift ratio. The behaviour beyond this level was similar to that of the unretrofitted specimen, and the failure occurred at 2% drift ratio. The hysteretic relationships recorded during the test are illustrated in Figure 18.

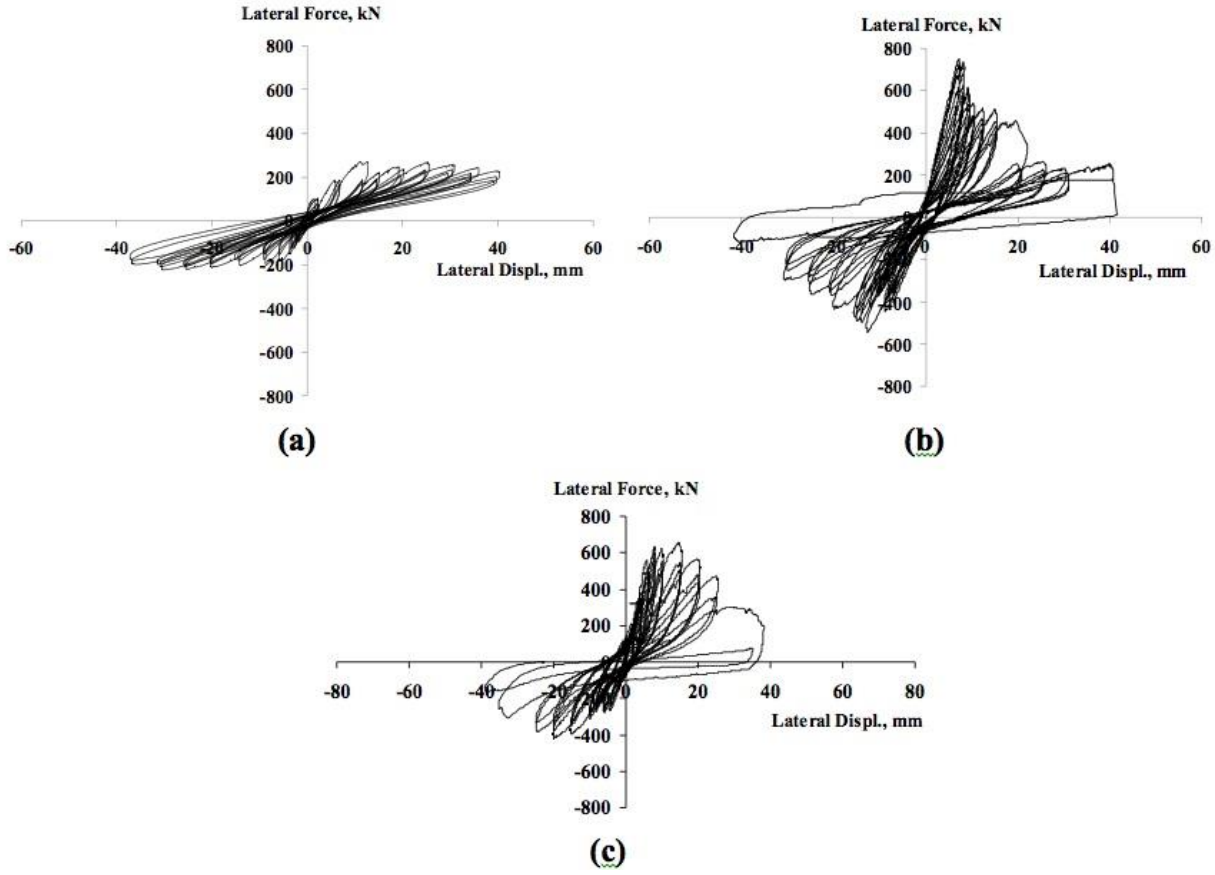

Fig. 18 – Hysteretic Relationships, (a) Unretrofitted (BL-1), (b) Retrofitted with CFRP Covering the entire wall Surface (BL-2), (c) Retrofitted with Diagonal CFRP strips (BL-3)

Specimen BL-3 initially behaved similar to BL-2. Test observations indicated no visible cracking during the initial cycles at 0.1% and 0.3% drift ratios. Some noise was heard during these initial load applications, indicating signs of local stretching and possible debonding from the blocks locally. However there was no sign of damage. The lateral drift ratio of 0.3% was attained at 558 kN and 278 kN of loading in the push and pull modes, respectively. The specimen remained essentially intact, without any serious damage, and continued resisting additional loads. Some local debonding and buckling of FRP strips was observed in compression, which subsequently had to stretch before it could develop full resistance. The maximum lateral load resistance occurred at 0.75 % lateral drift ratio during pushing, and was equal to 659 kN. The improvement in load resistance due to retrofitting resulted in 2.4 times the lateral load resistance recorded in unretrofitted specimen (659/273). The maximum strain in FRP occurred when the maximum load resistance of the specimen was attained and was measured to be 5300 micro strains at the centre of the bottom corner of FRP strip. The specimen sustained somewhat lower resistance when pulled, developing 424 kN of resistance at 1.0 % drift ratio. This was attributed to local debonding and buckling of strips in compression during the initial load excursion, which resulted in reduced load resistance upon load reversal. However the FRP remained well anchored to the surrounding frame elements because of the FRP anchors used.

The hysteretic relationships indicated that there was no significant improvement in deformability beyond 0.5% lateral drift, which corresponded to the onset of FRP rupturing followed by column failure at about 1% lateral drift, because of column splice failures as typically observed in older frames. This observation indicates that the seismic retrofit strategy for non-ductile frame wall assemblies should be based on elastic design, unless individual frame members are retrofitted for improved deformability. A single layer of CFRP strips of 625 mm wide and 0.9 mm thick (after impregnation in epoxy to form a composite

material) on both sides of the masonry wall (with 700 MPa coupon strength) was sufficient to increase the elastic load resistance by about 2.5 times in the direction of original load excursion and by about 2.0 upon load reversal. Analysis of the frame-wall assembly with a simple analytical model, consisting of flexural frame elements, a diagonal strut for the masonry wall and a diagonal tie for the FRP strip produced fairly accurate capacity calculations in the original direction of loading. It may be prudent to reduce the effectiveness of FRP ties by a factor of 2.0 to account for the possibility of debonding and resulting local fiber buckling in compression before they are subjected to tension under reversed cyclic loading. Further research is needed to establish the characteristics of FRP sheets bonded on masonry walls under reversed cyclic loading.

3.3. Out-of-Plane Stability of URM Walls

A comprehensive experimental and analytical research project was conducted at the Earthquake Engineering Research Facility (EERF) of the University of British Columbia (Penner 2014; Penner and Elwood, 2015a; Penner and Elwood, 2015). The objective of research was to assess the dynamic one-way out-of-plane bending response of URM walls connected to flexible supports. Full-scale shake table tests were conducted with varying support flexibilities. A total of five was specimens were constructed and tested. Figure 19 illustrates the wall geometry and Fig. 20 shows a typical wall specimen prior to testing. The walls were tested using the single degree of freedom shake table in the EERF. The tests were conducted using two ground motion records, with one motion selected for significant long period spectral response (recorded during the February 22, 2011 Christchurch Earthquake) and the other for a dominant short-period spectral response (recorded during the October 18, 1989 Loma Prieta Earthquake).

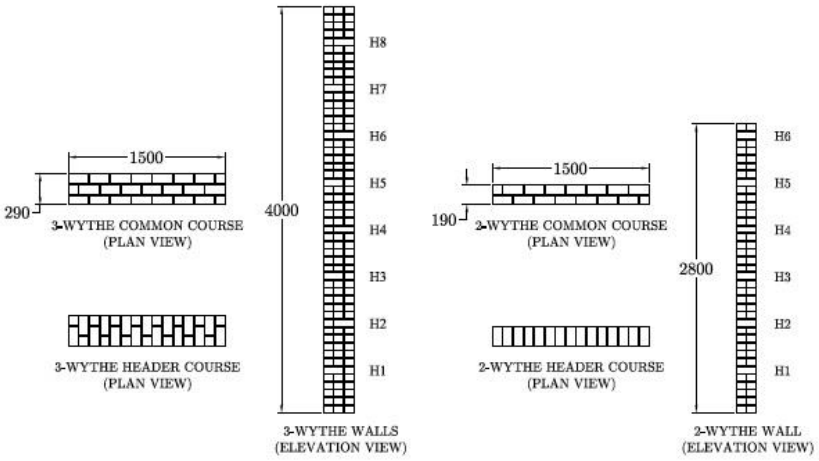

Fig. 19 Wall Geometry (Penner 2014)

Fig. 20 Typical Wall Specimen Prior to Testing (Penner 2014)

The wall specimens were supported through coil springs at the top and bottom to simulate the flexibility of floor diaphragms. The test variables included diaphragm stiffness and wall height. Walls were first subjected to cracking ground motions with rigid diaphragms. They were then tested to failure with flexible diaphragms. All walls sustained horizontal cracks at about their mid-heights. The ground motion intensity varied with boundary conditions. The lowest collapse condition was obtained under 60% of the as-recorded amplitude, while the highest was about twice this level. Flexible diaphragms resulted in higher motion intensities. The wall tested with rigid diaphragms showed lowest intensity at collapse. This wall also experienced the highest rocking prior to collapse. The walls with a flexible top diaphragm and rigid bottom diaphragm showed virtually no rocking until collapse, though they withstood the highest intensity of ground motion. The force demands at the top and bottom in stable runs were about 50% higher than those predicted by the use of the spectral acceleration of the input motion and the period of the system. Demands on the bottom connection were consistently higher than those on the top connection.

The research project was then extended to the analytical phase. The shake table tests were used to validate a computational model. The analytical investigation had the objective of examining the effects of selected wall and ground motion parameters. Further details on the research project can be obtained elsewhere (Penner 2014; Penner and Elwood, 2015a; Penner and Elwood, 2015).

4. Summary and Conclusions

A review of the seismic evaluation process provided in ASCE41-13 is made, with particular emphasis on masonry buildings. It is pointed out that those building that do not meet the Performance Objectives specified in the standard may have to be retrofitted for improved strength and deformability. A number of research projects, conducted within the scope of the Canadian Seismic Research Network, addressing masonry performance under seismic loading, including new retrofit techniques recently developed within the Network, are reviewed. It is shown that shear deficient load bearing masonry walls can be strengthened by surface mounted CFRP sheets. CFRP laminates control diagonal tension cracking, while also improving diagonal compression capacity of masonry. Flexural capacities of masonry walls can be improved by properly anchoring surface mounted CFRP to the supporting element (foundation in the wall tests reported herein). The use of stainless steel sheet anchors, as well as CFRP anchors result in significant enhancements in flexural capacities. The former also results in ductile response. Full-size shake table tests indicate that diaphragm flexibility affects wall out-of-place behaviour significantly, increasing force demands at top and bottom connections.

5. Acknowledgements

The authors greatly acknowledge the funding of the Canadian Seismic Research Network provided by the Natural Sciences and Engineering Research Council of Canada.

6. References

ARIFUZZAMAN, Shah, Seismic Retrofit of Load Bearing Masonry Walls with Surface Bonded FRP Sheets'', Master of Applied Science Thesis, Department of Civil Engineering, University of Ottawa, 2013, 162 p.

ASCE, ASCE/SEI 41-13, "Seismic Evaluation and Retrofit of Existing Buildings", American Society of Civil Engineers, 2013, 518 p.

NATIONAL RESEARCH COUNCIL OF CANADA, "National Building Code of Canada", 2010, Ottawa, Canada.

OZBAKKALOGLU, Togay and SAATCIOGLU, Murat, "Tensile Behavior of FRP Anchors in Concrete," *ASCE Journal of Composites*, 13(2), pp. 82-92, 2009.

PENNER, Osmar, "Out-of Plane Dynamic Stability of Unreinforced Masonry Walls Connected to Flexible Diaphragms", PhD Dissertation, *University of British Columbia*, 2014, 387 p.

PENNER, Osman and ELWOOD, Ken, "Out-of-plane Dynamic Stability of Unreinforced Masonry Walls: Shake Table Testing", *Earthquake Spectra* (in print), 2015a.

PENNER, Osman and ELWOOD, Ken, "Out-of-plane Dynamic Stability of Unreinforced Masonry Walls: Parametric Study and Assessment of Guidelines", *Earthquake Spectra* (in print), 2015b.

SAATCIOGLU, Murat, SERRATO, Fabio and FOO, Simon. "Seismic performance of masonry infill walls retrofitted with CFRP sheets", *Proceedings of the 7th International Symposium on Fiber Reinforced Polymer Reinforcement for Reinforced Concrete Structures (FRPRCS-7),* American Concrete Institute, 2005.

TAGHDI, Mustafa, BRUNEAU, M. and SAATCIOGLU, Murat, "Seismic Retrofitting of Low-Rise Masonry and Concrete Walls Using Steel Strips", ASCE Journal of Structural Engineering, 126(9), pp.1017-1025, 2000.